Provisioning Short-Term Traffic Fluctuations in Elastic Optical Networks

Zhizhen Zhong, *Student Member, IEEE*, Nan Hua, *Member, IEEE*, Massimo Tornatore, *Senior Member, IEEE*, Jialong Li, Yanhe Li, Xiaoping Zheng, and Biswanath Mukherjee, *Fellow, IEEE*

***Abstract*— Transient traffic spikes are becoming a crucial challenge for network operators from both user-experience and network-maintenance perspectives. Different from long-term traffic growth, the bursty nature of short-term traffic fluctuations makes it difficult to be provisioned effectively. Luckily, next-generation elastic optical networks (EONs) provide an economical way to deal with such short-term traffic fluctuations. In this paper, we go beyond conventional network reconfiguration approaches by proposing the novel lightpath-splitting scheme in EONs. In lightpath splitting, we introduce the concept of Split-Points to describe how lightpath splitting is performed. Lightpaths traversing multiple nodes in the optical layer can be split into shorter ones by SplitPoints to serve more traffic demands by raising signal modulation levels of lightpaths accordingly. We formulate the problem into a mathematical optimization model and linearize it into an integer linear program (ILP). We solve the optimization model on a small network instance and design scalable heuristic algorithms based on greedy and simulated annealing approaches. Numerical results show the tradeoff between throughput gain and negative impacts like traffic interruptions. Especially, by selecting SplitPoints wisely, operators can achieve almost twice as much throughput as conventional schemes without lightpath splitting.**

***Index Terms*— Network reconfiguration, traffic fluctuations, elastic optical networks, lightpath splitting, network optimization.**

I. Introduction

IS RUNNING the network with much excess capacity the only effective way to accommodate sudden and short-term traffic fluctuations? Surely, a larger capacity means less congestion, and more requests can be served, leading to improved user experience and higher income. Unfortunately, adding more network capacity will increase both Capital Expenditures (CapEx) and Operational Expenditures (OpEx). Conventional network management schemes are based on the assumption that spikes during traffic fluctuations are not so severe, which was indeed true in the past. Hence, a common way to accommodate traffic fluctuations consisted in dimensioning network capacity based on traffic spikes [1], [2], and turning some network equipment on/off following traffic fluctuations [3]–[6].

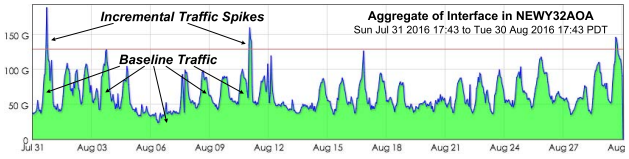

Fig. 1. Aggregated traffic fluctuations of New York in Internet2 network (accessed 30 Aug 2016 PDT, via http://snapp2.bldc.grnoc.iu.edu/i2net/).

Traffic is now becoming more dynamic and bursty than ever before, and this observation motivates operators to revisit the problem of how to effectively accommodate traffic fluctuations. Today, traffic fluctuations with extremely sharp spikes may require bandwidth many times beyond baseline traffic amount, or even several times beyond normal maximum traffic. Two examples illustrate this trend. The first is a recent game, Pokemon GO, which generated traffic 50 times beyond expectations [7], showing how unexpectedly new traffic spikes can occur in the network. Also, specific nation- or world-wide mega events, like Double Eleven in China, Black Friday in the U.S. [8], [9], finals of FIFA World Cup, and Olympic Games [10], induce severe traffic spikes. These spikes are generated by millions of users standing out of their daily habits, and usually last for only few hours, or days. Fig. 1 shows an example on how incremental traffic spikes overload the network (50% more than baseline peaks, 200% more than baseline valleys) in a low frequency (twice a month).

Therefore, operators must address a complex tradeoff between service quality at traffic spikes and network cost: *on one hand, providing high performance even in case of occasional sharp spikes requires much larger capacity (over-equipped for most of time, and leading to higher CapEx and OpEx); on the other hand, more conservative capacity dimensioning does not allow to serve traffic spikes effectively (service outages in spike hour may negatively affect subscribers' loyalty)*. Conventional strategies based on turning off idle equipment in a over-provisioned network cannot solve this problem completely, because they can only reduce electricity costs (a part of OpEx), while other parts of OpEx, such as human-resource cost, and CapEx will not be saved. Also, frequent on-off operations driven by daily fluctuations might deteriorate equipment lifetime, leading to high repair cost (OpEx) or need for premature investment on new infrastructures (CapEx) [11]–[13]. Thus, new methods are

Manuscript received March 6, 2018; revised December 27, 2018; accepted May 28, 2019; approved by IEEE/ACM TRANSACTIONS ON NETWORKING Editor S. Subramaniam. Date of publication July 22, 2019; date of current version August 16, 2019. This work was supported in part by the NSFC under Grant 61871448 and Grant 61621064, in part by the National Science Foundation under Grant 1716945, and in part by the Networks Lab., UC Davis. *(Corresponding author: Xiaoping Zheng.)*

Z. Zhong, N. Hua, J. Li, Y. Li, and X. Zheng are with the Beijing National Research Center for Information Science and Technology, Department of Electronic Engineering, Tsinghua University, Beijing 100084, China (e-mail: xpzheng@mail.tsinghua.edu.cn).

M. Tornatore is with the Department of Electronics, Information and Bioengineering, Politecnico di Milano, 20133 Milan, Italy, and also with the Networks Lab., University of California at Davis, Davis, CA 95616 USA.

B. Mukherjee is with the Networks Lab., University of California at Davis, Davis, CA 95616 USA.

Digital Object Identifier 10.1109/TNET.2019.2925631

needed to handle such short-term traffic fluctuations. And this is what we aim to address throughout this study.

In this work, we present a comprehensive study on provisioning short-term traffic fluctuations under a novel network reconfiguration scheme with lightpath splitting. We summarize our contributions as follows: 1) to the best of our knowledge, this is the first work on provisioning short-term traffic fluctuations in Elastic Optical Networks (EONs) via optical-layer reconfigurations; 2) a novel network reconfiguration scheme with lightpath splitting is devised; 3) we formulate the problem using a mathematical model and acquire its results to guide the design of scalable algorithms; and 4) both greedy and simulated annealing algorithms are proposed to quickly solve the problem. Illustrative results show that we can achieve significant throughput improvement by affecting a fraction of traffic due to reconfiguration under incremental traffic spikes.

The remainder of the study is organized as follows: Section II discusses the role of short-term reconfiguration, and reviews prior works. Section III introduces the lightpath-splitting scheme. Section IV mathematically formulates the problem of lightpath splitting, and obtains its optimization results. Section V devises scalable heuristic algorithms for large network instances. Section VI presents illustrative numerical evaluations by simulation. Section VII concludes this study.

II. Short-Term Reconfigurations for Network Maintenance and Management

A. Role of Short-Term Reconfigurations

We divide short-term traffic fluctuations into two parts: baseline traffic and incremental traffic spikes, as depicted in Fig. 1. Baseline traffic refers to the average daily traffic, while incremental traffic spikes are transient load increases.

Generally, network capacity is sufficient for baseline traffic, and lightpaths are provisioned in a relatively static way (weeks or months without change). If a traffic spike arrives, the network monitor in charge of detecting traffic anomaly [14] will trigger short-term network re-planning and reconfiguration (inner cycle in Fig. 2) based on current network planning result (see the arrow directed from network planning to short-term network re-planning). When short-term spikes leave, those split lightpaths will gradually recover to original longer lightpaths. The details on the recovery process are out of the scope of this paper, and we only discuss spikes provisioning.

Note that short-term reconfiguration is intended as an emergency plan for operators to avoid short-term resource crunch. For longer-term traffic growth, usual periodic network capacity upgrade (outer cycle in Fig. 2) that scales networks out by adding new equipments is important and necessary [15], [16].

B. Related Work

Many conventional investigations on short-term reconfigurations focused on the energy efficiency gain in a over-provisioned network. Reference [3] presented a strategy to save energy consumption when traffic varies. Reference [4] employed lightpath bypass and router-card sleep modes to minimize energy consumption under daily traffic fluctuation. Reference [5] compared various traffic-aware strategies for energy efficiency. Reference [17] proposed a power-aware traffic management protocol to reduce overheads. Other studies consider the tradeoff between energy efficiency and device lifetime [11]–[13].

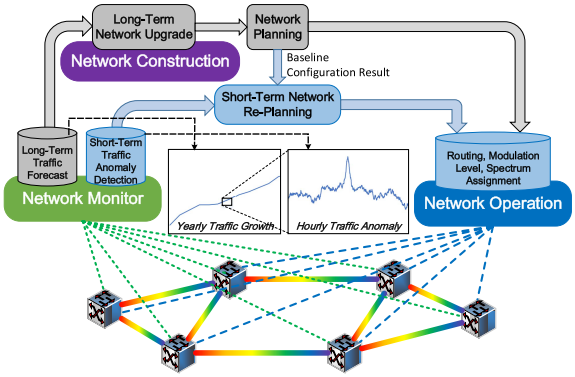

Fig. 2. Short-term reconfigurations in network maintance and management.

Regarding short-term reconfigurations to avoid network congestion, [2] proposed a technique that leveraged a small amount of link capacity to achieve high resource utilization without congestion. Reference [18] studied both short-term traffic variation and long-term traffic growth, and concluded that network re-optimization without optical path re-routing and wavelength defragmentation does not lead to significant performance improvement. This work inspires us to serve traffic fluctuations by optical-layer reconfigurations [19]–[22].

The idea of splitting optical-layer long lightpaths into shorter ones was discussed in [23] for Wavelength-Division-Multiplexed (WDM) networks. Lightpath splitting as a way of network reconfiguration was studied in WDM ring networks with a simple heuristic algorithm [24]. Reference [25] showed that short lightpaths can achieve higher resource utilization and lower blocking probability. In EONs, shorter lightpaths can support higher-order modulations, which in turn increase network capacity [26]. This fact inspires us to devise a solution to exploit the elasticity of the optical layer to accommodate incremental traffic spikes [27], [28]. Experiments also supports quick modulation format reconfiguration [29]–[31].

Different from the above methods that reconfigure network hardware, degraded service provisioning acts as the admission control for bandwidth reconfiguration. The main point for degraded service provisioning lies in the idea that a degraded level of service can be provided (instead of no service at all) when the network becomes congested [32]–[36]. On the joint reconfiguration of both traffic bandwidth and network infrastructures, Reference [37] explored multi-layer degraded service provisioning in EONs. Note that our method benefits from all these previous studies, which inspired us to conceive the idea of lightpath splitting [23]–[28], [32]–[37], as well as to support the feasibility of our approach [29]–[31]. In short, the core contribution of this study with respect to the existing body of literature is the introduction and comprehensive evaluation of lightpath-splitting concept as an amendment of network reconfiguration in EONs to cope with resource crunch during traffic spikes.

III. Lightpath Splitting Scheme

A. Principle and Definitions

We consider a network topology in a unidirectional graph: $\mathbf{G}(\mathbf{N}, \mathbf{E})$, where $\mathbf{N}$ and $\mathbf{E}$ denote the set of nodes and fiber

links, respectively. Lightpath l runs through nodes $\mathbf{N}_O(l)$ and links $\mathbf{E}_O(l)$ on optical layer, $\mathbf{N}_O(l) \subseteq \mathbf{N}$, $\mathbf{E}_O(l) \subseteq \mathbf{E}$. $S(l)$, $W(l)$, $L(l)$ represent the modulation level (in bits per symbol), number of adopted spectrum slots, and length, respectively, of lightpath l. F is the total number of spectrum slots of a fiber. The transparent reach of modulation level $S(l)$ is $T[S(l)]$.

Definition 1 (SplitPoint): A ***SplitPoint*** *on lightpath l is defined as a tuple $V_i = [v, l]$, $v \in \mathbf{N}_O(l)$, so that l is split into two segments, l_1, l_2, by V_i. In this case, we have $\mathbf{N}_O(l_1) \subsetneq \mathbf{N}_O(l)$, $\mathbf{N}_O(l_2) \subsetneq \mathbf{N}_O(l)$, $\mathbf{N}_O(l_1) \cap \mathbf{N}_O(l_2) = \{v\}$, $\mathbf{N}_O(l_1) \cup \mathbf{N}_O(l_2) = \mathbf{N}_O(l)$, and $\mathbf{E}_O(l_1) \subsetneq \mathbf{E}_O(l)$, $\mathbf{E}_O(l_2) \subsetneq \mathbf{E}_O(l)$, $\mathbf{E}_O(l_1) \cap \mathbf{E}_O(l_2) = \emptyset$, $\mathbf{E}_O(l_1) \cup \mathbf{E}_O(l_2) = \mathbf{E}_O(l)$.*

Definition 2 (SplitLightpath & PostSplitLightpath): If lightpath l is split into l_1 and l_2 by a SplitPoint $V_i = [v, l]$, l is a ***SplitLightpath****, and l_1 and l_2 are* ***PostSplitLightpaths****.*

Definition 3 (Lightpath Splitting): Lightpath splitting is performed when there are SplitPoints on SplitLightpaths. During lightpath splitting, the optical-layer route of the SplitLightpath is unchanged, while its adopted spectrum slots can be returned. After lightpath splitting, the modulation level and data rate of PostSplitLightpaths are guaranteed to not decrease. $S(l)W(l) \leq S(l_1)W(l_1)$ and $S(l)W(l) \leq S(l_2)W(l_2)$.

We define two policies for spectrum reallocation of PostSplitLightpaths: the first aims at maximizing electrical-layer capacity, named "MaxE", which only raises modulation levels of corresponding lightpaths, without shrinking the number of adopted spectrum slots. The other one aims at maximizing post-split optical-layer capacity, called "MaxO", which raises modulation levels while shrinking the number of adopted spectrum slots. During PostSplitLightpaths spectrum allocation, all available slots are equally likely to be utilized as long as they meet the spectrum continuity and contiguity constraints.

Theorem 1: For a SplitLightpath l and its PostSplitLightpaths l_1 and l_2, we have $Max\{S(l_1), S(l_2)\} > S(l)$ and $Min\{S(l_1), S(l_2)\} \geq S(l)$, under half-distance law[1] of optical signal transparent reach [26], [38], [39].

Proof: Based on optical signal transparent reach, we have $T[S(l)+1] < L(l) \leq T[S(l)]$. Half-distance law ensures $T[S(l)] = 2T[S(l)+1]$, so $T[S(l)+1] < L(l) \leq 2T[S(l)+1]$. Based on Definitions 1-3, $L(l) = L(l_1) + L(l_2)$.

If $L(l_1) > T(S(l)+1)$, $S(l_1) = S(l)$. Then, $L(l_2) < L(l) - T[S(l)+1] \leq T[S(l)+1]$, $S(l_2) \geq S(l)+1 > S(l)$. If $L(l_1) \leq T[S(l)+1]$, $S(l_1) \geq S(l)+1 > S(l)$. Then, $L(l_2) = L(l) - L(l_1) < L(l)$, $S(l_2) \geq S(l)$. Theorem 1 proved. □

We use a simple example to illustrate how lightpath splitting works. As shown in Fig. 3, SplitLightpath A-C originally traverses Fibers A-B and B-C with four slots under BPSK. If Node B is set to be a SplitPoint, then A-C is split into PostSplitLightpath A-B under 16QAM, and PostSplitLightpath B-C under QPSK (MaxE does not shrink the spectrum, while MaxO does, and both policies may retune the used spectrum slots). During this process, optical-layer route is not changed.

[1]Though many experiments have skewed this law by demonstrating higher-order modulation in a longer reach, the universal principle that higher-order modulation signal propagates shorter reach is true. Here, half-distance law acts as a well-known and generic mathematical relationship between transmission reach and modulation level only used to perform theoretical investigations.

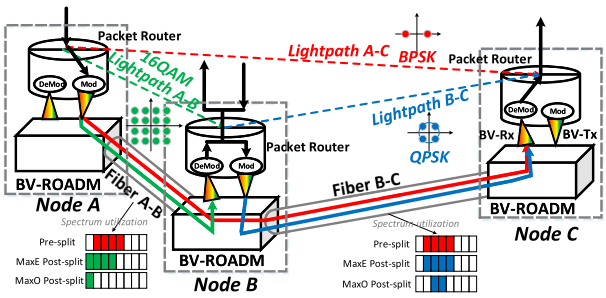

Fig. 3. Illustration of lightpath splitting.

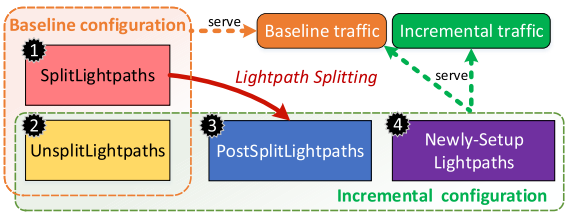

Fig. 4. Conceptual relationships among different kinds of lightpaths.

B. Relationships of Lightpaths

We explain the conceptual relationships among different lightpaths in the process of lightpath splitting in Fig. 4. Most of the time, operators run their network in baseline configuration. When traffic spike arrives, lightpath splitting is triggered. A fraction of baseline lightpaths are selected to become SplitLightpaths, and they are then split to be PostSplitLightpaths, while the remainder of baseline lightpaths, named UnsplitLightpaths, operate as before. Some lightpath splitting operations, like MaxO, can release occupied spectrum slots, which enables new lightpaths, i.e., Newly-Setup Lightpaths, to be established. The combination of UnsplitLightpaths, PostSplitLightpaths, and Newly-Setup Lightpaths makes up new network configuration under traffic spikes.

C. Capacity Improvement

We define function $\mathcal{F}(l) = S(l)W(l) + S_{max}[F - W(l)]$, as the capacity[2] of the fiber supporting lightpath l.

Theorem 2: Lightpath splitting can increase the total capacity of fiber links, which means: $Max\{\mathcal{F}(l_1), \mathcal{F}(l_2)\} > \mathcal{F}(l)$ and $Min\{\mathcal{F}(l_1), \mathcal{F}(l_2)\} \geq \mathcal{F}(l)$.

Proof: We build our proof on Theorem 1. For MaxO, we have:

If $L(l_1) > T(S(l)+1)$, we have $S(l_1) = S(l)$ and $S(l_2) > S(l)$. As $S(l_1) = S(l)$, so, $W(l_1) = W(l)$ and $\mathcal{F}(l_1) = \mathcal{F}(l)$. As $S(l_2) > S(l)$, $\frac{W(l)S(l)}{S(l_2)} \leq W(l_2)$, and $\mathcal{F}(l_2) = S_{max}F + W(l_2)[S(l_2) - S_{max}]$. We replace $W(l_2)$ and $S(l_2)$, and we have $\mathcal{F}(l_2) > S_{max}F + W(l)S(l) - W(l)S_{max} = \mathcal{F}(l)$.

If $L(l_1) \leq T[S(l)+1]$, we have $S(l_1) > S(l)$ and $S(l_2) \geq S(l)$. Besides, $W(l_1) \geq \frac{W(l)S(l)}{S(l_1)}$, $W(l_2) \geq \frac{W(l)S(l)}{S(l_2)}$. We put the above four inequalities into the expansions of $\mathcal{F}(l_1)$ and $\mathcal{F}(l_2)$, then, we have $\mathcal{F}(l_1) > \mathcal{F}(l)$ and $\mathcal{F}(l_2) \geq \mathcal{F}(l)$.

For MaxE, $W(l) = W(l_1) = W(l_2)$. Theorem 1 can be extended to prove Theorem 2. □

[2]The total capacity of a physical link, i.e., fiber, can be evaluated by the theoretical maximum amount of data that it can support [40]. Here, we consider this capacity to consist of two parts: utilized spectrum for lightpaths, and non-utilized spectrum. For non-utilized spectrum, we treat it as a potential resource and use the highest modulation level available.

Note that network capacity is a static concept, which is summed up by capacities of links, while network throughput is a dynamic concept from user perspectives, jointly decided by network capacity, network resource allocation schemes, and offered traffic requests. In real networks where traffic bandwidth granularities are much smaller than link capacity, network capacity becomes the dominant factor for network throughput. Therefore, the capacity improvement by lightpath splitting can increase network throughput.

D. Prerequisites and Applicabilities

As a network reconfiguration scheme, the effectiveness of lightpath splitting partly relies on baseline network configurations. To apply lightpath splitting, there are two prerequisites on lightpaths and transceivers.

Assumption 1: To perform lightpath splitting, each network node should be equipped with enough transceivers.

As we discussed, each added SplitPoint needs a pair of transceivers inside that node. In fact, operators usually equip extra transceivers at all nodes for backup or protection purposes, and the number of transceivers is not a constraint.

Assumption 2: To perform lightpath splitting, lightpaths in baseline configuration should have the potential to be split.

Here, "*the potential to be split*" means that a baseline lightpath l should be multi-hop in physical layer ($|\mathbf{N}_O(l)| > 2$). On modulation levels, if $S(l)$ is already in the highest modulation level and cannot be raised, the effect of modulation level increase will not be revealed, and problem then degenerates into existing ones that simply splitting long lightpaths into shorter ones for better resource flexibility [22]–[25]. In practical backbone networks, there will always be some lightpaths that traverse multiple physical nodes with thousands of kilometers long, and cannot use the highest modulation.

E. Negative Impacts

The negative impacts of lightpath splitting are from two perspectives: in-operation impacts and post-operation impacts.

During lightpath splitting, the main negative impact is the disruption of existing traffic. Specifically, traffic interruptions are caused by tearing down SplitLightpaths and setting up PostSplitLightpaths. The most critical barrier during lightpath addition and removal is the optical power instability caused by wavelength-dependent power excursions of the erbium-doped fiber amplifiers (EDFA) which are used for signal amplification in optical networks [41]. Detailed discussions of EDFA power fluctuations can be found in [42]–[44]. There are several existing techniques to mitigate the power excursions and reduce the power adjustment delay [45]–[49]. With these methods, the execution of lightpath splitting, which removes SplitLightpaths and adds PostSplitLightpaths, can be done within several seconds [44].

Note also that service interruption can be avoided by performing lightpath splitting in advance with proper scheduling algorithms [50]. Such beforehand operations are feasible because the traffic spikes are typically caused by pre-scheduled mega-events, which give operators enough time to perform lightpath splitting before traffic spikes arrive. Another positive aspect is that the baseline network is not fully-occupied, and usually has certain amount of spare network capacities to perform hitless capacity configuration by migrating the original traffic from SplitLightpaths to a backup path until lightpath splitting is complete [31] using dependency graphs [51] in a consistent manner. In these ways, the service interruption during lightpath splitting can be alleviated or even eliminated.

After lightpath splitting, the main negative impacts are degradation of end-to-end service latency,[3] and increase of energy consumption, deriving from the fact that traffic requests have to traverse shorter lightpaths (hence more transceivers) on average. It is worth reminding that the number of increased transceivers is equal to twice the number of SplitPoints.

IV. Formulations of Lightpath Splitting

Lightpath splitting, as a short-term reconfiguration, is performed in a provisioned network that is facing traffic spikes. The baseline lightpaths are set as the input.

A. The Mathematical Optimization Model

Here, we formulate a mathematical model to serve incremental traffic spikes on baseline network configurations (already provisioned). As stated before, the routes of baseline traffic (on both electrical and optical layers) cannot be changed, while it is only the modulation level along with spectrum allocation on optical layer that can be reconfigured.

General Parameters:

- $\mathbf{G}(\mathbf{N}, \mathbf{E})$, $T(a)$, F: as defined in Section III.A.
- $\mathbf{A}$: set of modulation levels a (in bits per symbol).
- $D(m, n)$: distance of fiber link (m, n).
- C: spectrum slot size (in Hz).
- M: a positive maximum number.
- $\mathbf{R}$: traffic set composed of $r = \{s_r, d_r, b_r\}$, which denotes a request's source, destination, and bandwidth, respectively.
- μ: scale parameter controlling the amount of incremental traffic spikes. So, the bandwidth of request r is $\mu \cdot b_r$
- η_1, η_2: scaling parameters for the objectives, $\eta_1 \gg \eta_2$.

Parameters for Baseline Lightpth Configurations:

- $\mathbf{L}$: set of baseline lightpaths[4] l.
- $\mathbf{E}_O(l)$, $\mathbf{N}_O(l)$, $S(l)$, $W(l)$: as defined in Section III.A.
- $H(l)$: physical-layer hops of baseline lightpath l.
- $B(l)$: occupied capacity by baseline traffic on baseline lightpath l, ensuring the route of baseline traffic is unchanged.

Binary Variables for Lightpath Splitting: $\forall (i, j) \in \mathbf{L}$, if (i, j) is an UnsplitLightpath, all variables below equal 0. But, its modulation level might be increased if necessary.

- $\pi_{(x,y)}^{(i,j)}$: equals 1 if SplitLightpath (i, j) is split into PostSplitLightpath (x, y).
- $\xi_{(m,n),f}^{(i,j),(x,y)}$: equals 1 if PostSplitLightpath (x, y) of SplitLightpath (i, j) uses fiber (m, n) on slot f.

[3] In optical networks, service latency mainly consists of propagation latency (0.005 ms/km) on optical layer, and nodal processing latency in packet routers on electrical layer for packet queuing, traffic grooming, signal multiplexing/demultiplexing at the end of lightpaths. Under the condition of optical-layer route unchanged, the number of traversed lightpaths (hops on electrical layer) is the decisive variable for request latency degradation.

[4] Note that a lightpath l can also be expressed as (i, j), where i and j denote source and destination, respectively, of the baseline lightpath.

- $\varphi^{(i,j)}_{(x,y),f}$: equals 1 if PostSplitLightpath (x,y) of SplitLightpath (i,j) employs slot f.
- $\omega^{(i,j)}_{(x,y),a}$: equals 1 if PostSplitLightpath (x,y) of SplitLightpath (i,j) uses modulation level a.

Binary Variables for Newly-Setup Lightpaths $(\tilde{i},\tilde{j})$

- $\alpha^{r}_{(\tilde{i},\tilde{j})}$: equals 1 if request r uses lightpath $(\tilde{i},\tilde{j})$ as an intermediate electrical-layer link.
- $\lambda^{(\tilde{i},\tilde{j})}_{(m,n),f}$: equals 1 if lightpath $(\tilde{i},\tilde{j})$ uses fiber link (m,n) on slot f.
- $\sigma^{(\tilde{i},\tilde{j})}_{(m,n)}$: equals 1 if lightpath $(\tilde{i},\tilde{j})$ uses fiber link (m,n).
- $\chi^{(\tilde{i},\tilde{j})}_{f}$: equals 1 if lightpath $(\tilde{i},\tilde{j})$ uses slot f.
- $\theta^{(\tilde{i},\tilde{j})}_{a}$: equals 1 if lightpath $(\tilde{i},\tilde{j})$ adopts modulation level a.

Variables for Incremental Traffic Accommodation: Here, if a request's bandwidth cannot be fully accessed, it is allowed to serve a fraction of the bandwidth.[5] So, we introduce $\rho_{\tilde{r}}$ as a bandwidth degradation indicator.

- ρ_r: integer, actual access bandwidth of request r under resource crunch, $0 \le \rho_r \le b_r$.
- ε_r: binary, equals 1 if request r is accessed.

Optimize: During traffic spikes, lightpath splitting is used by the operator to maximize the network throughput as a primary goal. As the introduction of SplitPoints poses negative impacts on existing traffic, the operator should try to avoid unnecessary SplitPoints to mitigate these impacts. Therefore, we maximize incremental network throughput first, and then minimize total number of SplitPoints second, as shown below.

$$\textbf{Maximize: } \eta_1 \cdot \sum_{r\in\mathbf{R}} \rho_r \cdot \varepsilon_r - \eta_2 \cdot \sum_{l\in L, x,y\in\mathbf{N}} \pi^{l}_{(x,y)}. \quad (1)$$

Constraints:

1) Optical-Layer Constraints for Lightpath Splitting:

$$\sum_{y\in\mathbf{N}_O(i,j)} \pi^{(i,j)}_{(x,y)} - \sum_{y\in\mathbf{N}_O(i,j)} \pi^{(i,j)}_{(y,x)} = \begin{cases} 1, & x=i \\ -1, & x=j \\ 0, & x\neq i,j, \end{cases} \quad \forall (i,j)\in L, x\in\mathbf{N}_O(i,j). \quad (2)$$

Eq. (2) is the lightpath splitting constraint deciding whether lightpath (i,j) is a SplitLightpath, and how to split it.

$$\pi^{l}_{(x,y)} = 0, \quad \forall l\in\mathbf{L}, x,y\in \complement_{\mathbf{N}}\mathbf{N}_O(i,j). \quad (3)$$

$$\sum_{f\in[1,W]} \varphi^{l}_{(x,y),f} = 0, \quad \forall l\in\mathbf{L}, x,y\in \complement_{\mathbf{N}}\mathbf{N}_O(i,j). \quad (4)$$

$$\sum_{a\in A} \omega^{l}_{(x,y),a} = 0, \quad \forall l\in\mathbf{L}, x,y\in \complement_{\mathbf{N}}\mathbf{N}_O(i,j). \quad (5)$$

$$\sum_{f\in[1,W]} \sum_{(m,n)\in\mathbf{E}} \xi^{l,(x,y)}_{(m,n),f} = 0, \quad \forall l\in\mathbf{L}, x,y\in \complement_{\mathbf{N}}\mathbf{N}_O(i,j). \quad (6)$$

$$\xi^{l,(x,y)}_{(m,n),f} = 0, \forall f\in[1,F], x,y\in\mathbf{N}, l\in\mathbf{L}, (m,n)\in\complement_{\mathbf{E}}\mathbf{E}_O(l). \quad (7)$$

[5]This electrical-layer bandwidth degradation [32]–[36] is set to fully exploit network capacity to overcome the drawback that served bandwidth of r is either 0 or b_r, due to discrete nature of ILP (ε_r is binary).

$$\sum_{(m,n)\in\mathbf{E}_O(l)} \xi^{l,(x,y)}_{(m,n),f} - \sum_{(n,m)\in\mathbf{E}_O(l)} \xi^{l,(x,y)}_{(n,m),f} = \begin{cases} \varphi^{l}_{(x,y),f}, & m=x \\ -\varphi^{l}_{(x,y),f}, & m=y \\ 0, & m\neq x,y, \end{cases} \quad \forall f\in[1,F], x,y\in\mathbf{N}, l\in\mathbf{L}. \quad (8)$$

$$1 \le \sum_{x,y\in\mathbf{N}} \pi^{l}_{(x,y)} \le H(l), \quad \forall l\in\mathbf{L}. \quad (9)$$

On PostSplitLightpaths routing, Eqs. (3)-(8) ensure that a SplitLightpath is split within its routed nodes set, which means that the optical-layer route is unchanged. Eq. (9) ensures the number of PostSplitLightpaths should be no larger than the number of original lightpath hops of the SplitLightpath.

$$\pi^{l}_{(x,y)} \le \sum_{f\in[1,W]} \varphi^{l}_{(x,y),f} \le M\cdot\pi^{l}_{(x,y)}, \quad \forall x,y\in\mathbf{N}, l\in\mathbf{L}. \quad (10)$$

$$-M\cdot(\varphi^{l}_{(x,y),f} - \varphi^{l}_{(x,y),f+1} - 1) \ge \sum_{f'\in[f+2,W]} \varphi^{l}_{(x,y),f'}, \quad \forall f\in[1,F-1], x,y\in\mathbf{N}, l\in\mathbf{L}. \quad (11)$$

On PostSplitLightpaths spectrum allocation, Eq. (10) triggers PostSplitLightpaths slot allocation if l is a SplitLightpath. Eq. (11) is spectrum-consecutive constraint.

$$\sum_{f\in[1,F]} \varphi^{l}_{(x,y),f} \cdot \sum_{a\in\mathbf{A}} a\cdot\omega^{l}_{(x,y),a} \ge W(l)\cdot S(l)\cdot\pi^{l}_{(x,y)}, \quad \forall l\in\mathbf{L}, x,y\in\mathbf{N}. \quad (12)$$

$$\sum_{a\in\mathbf{A}} a\cdot\omega^{l}_{(x,y),a} \ge S(l)\cdot\pi^{l}_{(x,y)}, \quad \forall l\in\mathbf{L}, x,y\in\mathbf{N}. \quad (13)$$

$$\sum_{f\in[1,F]} \varphi^{l}_{(x,y),f} \le W(l), \quad \forall l\in\mathbf{L}, x,y\in\mathbf{N}. \quad (14)$$

$$\sum_{a\in\mathbf{A}} \omega^{l}_{(x,y),a} \le 1, \quad \forall l\in\mathbf{L}, x,y\in\mathbf{N}. \quad (15)$$

$$\pi^{l}_{(x,y)} \le \sum_{a\in\mathbf{A}} \omega^{l}_{(x,y),a} \le M\cdot\pi^{l}_{(x,y)}, \quad \forall x,y\in\mathbf{N}, l\in\mathbf{L}. \quad (16)$$

$$\sum_{(m,n)\in\mathbf{E}} \xi^{l,(x,y)}_{(m,n),f} \cdot D(m,n) \le T(a) - M\cdot(\omega^{l}_{(x,y),a} - 1), \quad \forall l\in\mathbf{L}, x,y\in\mathbf{N}, a\in\mathbf{A}, f\in[1,F]. \quad (17)$$

$$\sum_{a\in\mathbf{A}} \omega^{l}_{(x,y),a} \le \sum_{f\in[1,F]} \varphi^{l}_{(x,y),f} \le M\cdot\sum_{a\in\mathbf{A}} \omega^{l}_{(x,y),a}, \quad \forall l\in\mathbf{L}, x,y\in\mathbf{N}. \quad (18)$$

On PostSplitLightpaths modulation level determination, Eqs. (12)-(14) ensure that PostSplitLightpaths have no larger spectrum usage, and no smaller data rate and modulation level than original ones. Eq. (15) ensures PostSplitLightpaths use only one modulation format. Eq. (16) reveals the relationship between modulation level allocation and lightpath splitting. Eq. (17) is PostSplitLightpath maximum-transmission-reach constraint. Eq. (18) describes the relationship between utilized modulation and occupied spectrum of PostSplitLightpaths.

2) Optical-Layer Constraints for Newly-Setup Lightpaths:

$$-M\cdot(\chi^{(\tilde{i},\tilde{j})}_{f} - \chi^{(\tilde{i},\tilde{j})}_{f+1} - 1) \ge \sum_{f'\in[f+2,W]} \chi^{(\tilde{i},\tilde{j})}_{f'}, \quad \forall \tilde{i},\tilde{j}\in\mathbf{N}, f\in[1,F-1]. \quad (19)$$

$$\sum_{n\in\mathbf{N}} \lambda^{(\tilde{i},\tilde{j})}_{(m,n),f} - \sum_{n\in\mathbf{N}} \lambda^{(\tilde{i},\tilde{j})}_{(n,m),f} = \begin{cases} \chi^{(\tilde{i},\tilde{j})}_f, & m=\tilde{i} \\ -\chi^{(\tilde{i},\tilde{j})}_f, & m=\tilde{j} \\ 0, & m\neq\tilde{i},\tilde{j}, \end{cases}$$
$$\forall f\in[1,F],\ \tilde{i},\tilde{j}\in\mathbf{N}. \quad (20)$$

$$\sum_{l\in\mathbf{L},x,y\in\mathbf{N}} \xi^{l,(x,y)}_{(m,n),f} + \sum_{\tilde{i},\tilde{j}\in N} \lambda^{(\tilde{i},\tilde{j})}_{(m,n),f} \leq 1,$$
$$\forall f\in[1,F],(m,n)\in\mathbf{E}. \quad (21)$$

$$\sigma^{(\tilde{i},\tilde{j})}_{(m,n)} \leq \sum_{f\in[1,F]} \lambda^{(\tilde{i},\tilde{j})}_{(m,n),f} \leq \sigma^{(\tilde{i},\tilde{j})}_{(m,n)} \cdot M,$$
$$\forall\tilde{i},\tilde{j}\in\mathbf{N},(m,n)\in\mathbf{E}. \quad (22)$$

$$\sum_{n\in\mathbf{N}} \sigma^{(\tilde{i},\tilde{j})}_{(m,n)} \leq 1, \quad \forall\tilde{i},\tilde{j},m\in\mathbf{N}. \quad (23)$$

$$\sum_{m\in\mathbf{N}} \sigma^{(\tilde{i},\tilde{j})}_{(m,n)} \leq 1, \quad \forall\tilde{i},\tilde{j},n\in\mathbf{N}. \quad (24)$$

$$\sigma^{(\tilde{i},\tilde{j})}_{(m,n)} + \sigma^{(\tilde{i},\tilde{j})}_{(n,m)} \leq 1, \quad \forall\tilde{i},\tilde{j},(m,n)\in\mathbf{E}. \quad (25)$$

$$\sum_{a\in\mathbf{A}} \theta^{(\tilde{i},\tilde{j})}_a \leq 1, \quad \forall\tilde{i},\tilde{j}\in\mathbf{N}. \quad (26)$$

$$\sum_{(m,n)\in\mathbf{E}} \lambda^{(\tilde{i},\tilde{j})}_{(m,n),f} \cdot D(m,n) \leq T(a) - M\cdot(\theta^{(\tilde{i},\tilde{j})}_a - 1),$$
$$\forall\tilde{i},\tilde{j}\in\mathbf{N},f\in[1,F],a\in\mathbf{A}. \quad (27)$$

$$\sum_{a\in\mathbf{A}} \theta^{(\tilde{i},\tilde{j})}_a \leq \sum_{f\in[1,F]} \chi^{(\tilde{i},\tilde{j})}_f \leq M\cdot\sum_{a\in\mathbf{A}} \theta^{(\tilde{i},\tilde{j})}_a, \quad \forall\tilde{i},\tilde{j}\in\mathbf{N}. \quad (28)$$

Eq. (19) ensures lightpaths' occupied spectrum slots should be consecutive. Eq. (20) is optical-layer flow-conservation constraint. Eq. (21) ensures a spectrum slot on a fiber can only be used once. Eq. (22) ensures that a fiber link is used when spectrum slots on this fiber are used. Eqs. (23)-(25) ensure that lightpaths are routed without loops. Eq. (26) ensures a lightpath adopts only one modulation format, and Eq. (27) is lightpaths' maximum transmission reach constraint. Eq. (28) formulates the relationship between utilized modulation and occupied spectrum of a lightpath.

3) Electrical-Layer Constraints for Traffic Spikes: Traffic spikes are provisioned over incremental network configurations, which are the combination of UnSplitLightpaths, PostSplitLightpaths and Newly-Setup Lightpaths, as depicted in Fig. 4. Therefore, (i,j) here represents the sum of all lightpaths capacities from node i to node j.

$$\sum_{j\in\mathbf{N}} \alpha^r_{(i,j)} - \sum_{j\in\mathbf{N}} \alpha^r_{(j,i)} = \begin{cases} \varepsilon_r, & i=s_r \\ -\varepsilon_r, & i=d_r \\ 0, & i\neq s_r,d_r, \end{cases} \quad \forall r\in\mathbf{R}. \quad (29)$$

$$\sum_{i\in\mathbf{N}} \alpha^r_{(i,j)} \leq 1, \quad \forall r\in\mathbf{R},j\in\mathbf{N}. \quad (30)$$

$$\sum_{j\in\mathbf{N}} \alpha^r_{(i,j)} \leq 1, \quad \forall r\in\mathbf{R},i\in\mathbf{N}. \quad (31)$$

$$\alpha^r_{(i,j)} + \alpha^r_{(j,i)} \leq 1, \quad \forall r\in\mathbf{R},i,j\in\mathbf{N}. \quad (32)$$

$$\rho_r \leq \mu\cdot b_r, \quad \forall r\in\mathbf{R}. \quad (33)$$

$$\varepsilon_r \leq \rho_r \leq M\cdot\varepsilon_r, \quad \forall r\in\mathbf{R}. \quad (34)$$

$$\sum_{r\in\mathbf{R}} \rho_r\cdot\alpha^r_{(i,j)} + \sum_{l\in\mathbf{L}} B(l)\cdot\pi^l_{(i,j)} \leq C\cdot\sum_{f\in[1,F]}\sum_{a\in\mathbf{A}} (\sum_{l\in\mathbf{L}} \varphi^l_{(i,j),f}\cdot a\cdot\omega^l_{(i,j),a} + \chi^{(i,j)}_f\cdot a\cdot\theta^{(i,j)}_a), \quad \forall i,j\in\mathbf{N}. \quad (35)$$

TABLE I
MODULATION FORMAT VS. DATA RATE VS. TRANSMISSION REACH

Modulation format	BPSK	QPSK	8QAM	16QAM
Bits per symbol (b/s/Hz)	1	2	3	4
Slot bandwidth (GHz)	12.5	12.5	12.5	12.5
Data rate (Gbps)	12.5	25	37.5	50
Transmission reach (km)	9600	4800	2400	1200

Eq. (29) is electrical-layer flow-conservation constraint. Eqs. (30)-(32) ensure that lightpaths are routed over a single path on optical layer without loops. Eq. (33) ensures that the actual access bandwidth should not exceed the original requested bandwidth. Eq. (34) shows when traffic is blocked. Eq. (35) is lightpath capacity constraint ensuring that the sum of served bandwidth of traffic spikes and baseline traffic can not exceed the sum capacity of UnSplitLightpaths, PostSplitLightpaths, and newly-setup lightpaths between node pair (i,j).

B. Model Linearization and Optimization Results

For non-linear constraints Eqs. (12), (35), we linearize them with auxiliary variables and constraints added.[6,7]

A relative small-scale 6-node topology (as shown in Fig. 5(a)) is adopted to evaluate the performance of our proposed optimization model. We run our optimization model by a commercial IBM CPLEX solver on a computer with 2.4 GHz CPU and 32 GB RAM.[8] All fibers are unidirectional with 20 spectrum slots, and width of each slot is 12.5 GHz.

On the input parameters, Table I summarizes the parameters of different modulation formats according to theoretical and experimental results that have demonstrated the tradeoff between transmission reach and modulation level [26], [52]–[57]. Table II shows the input traffic profile as well as configurations of baseline lightpaths. Under the condition that all baseline traffic is served, we start with low modulation levels first, and increase modulation levels as the amount of traffic spike increases before lightpath splitting. Note also that the effectiveness of lightpath splitting does not rely on these specific data. As long as the two prerequisites in Section III.D can be satisfied, similar performance can be yielded.

Two benchmark experiments are conducted as comparisons. One is named *all lightpath splitting*, which means that all intermediate nodes of baseline lightpaths are set to be SplitPoints. The other is called *without lightpath splitting*, which means lightpath splitting is not performed, and the traffic spikes is

[6]Linearization for the product c of two binary variables a, b. c is also a binary variable, $c=a\cdot b$, subject to: $c\geq a+b-1,\ c\leq a,\ c\leq b$.

[7]Linearization for the product of a binary variable x and a integer variable y: we assume that y has a set of its possible integer values $Y=\{w_i\}$ $(1\leq i\leq n_Y)$, where w_i is a parameter, and n_Y is the size of Y. Then, we define a binary variable z_i, subject to: $y=w_i\cdot z_i,\ \forall i\in[1,n_Y]$. Therefore, the product, $x\cdot y$ can be expressed as the product of two binary variables, thus it can be further linearized with the method in footnote 6.

[8]Not all runs finished their optimization, so we further set a maximum running time of 72 hours, and a relative gap tolerance of 0.01 between best integer and best bound in the solver. The solver will finish its calculation and return results if either criterion is reached.

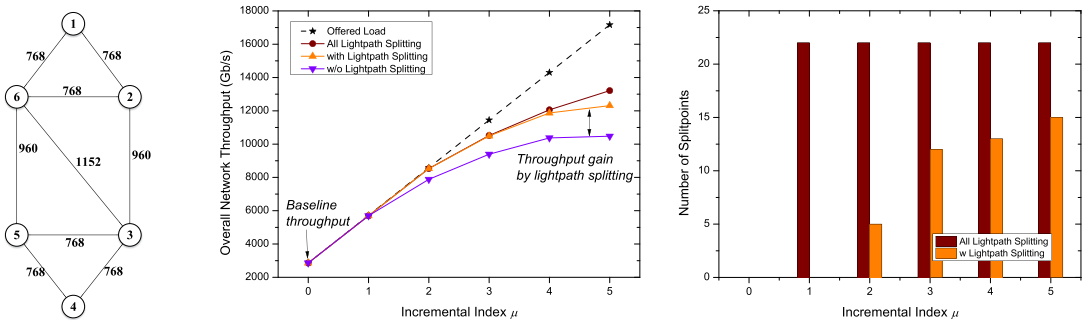

(a) 6-node topology. (b) Overall network throughput. (c) Number of SplitPoints..

Fig. 5. Optimization topology and results.

TABLE II

INPUTS: BASELINE LIGHTPATHS CONFIGURATIONS AND BASELINE TRAFFIC PROFILE (TOTAL AMOUNT = 2861 Gb/s)

Baseline Lightpaths l	$S(l)$ (b/s/Hz)	$W(l)$ (GHz)	$B(l)$ (Gb/s)	Supporting requests r
(1,2)	2	112.5	185	(1,2,185)
(1,6,3)	1	112.5	103	(1,3,103)
(1,6,3,5,4)	1	50	47	(1,4,47)
(1,6,5)	1	87.5	71	(1,5,71)
(1,2,3,6)	2	100	195	(1,6,195)
(2,1)	1	162.5	155	(2,1,155)
(2,3)	1	100	93	(2,3,93)
(2,3,4)	1	37.5	37	(2,4,37)
(2,6,5)	1	37.5	24	(2,5,24)
(2,6)	1	137.5	130	(2,6,130)
(3,2,1)	1	37.5	33	(3,1,33)
(3,2)	1	12.5	2.5	(3,2,2.5)
(3,4)	1	200	151	(3,4,151)
(3,5)	1	200	174	(3,5,174)
(3,2,6)	1	50	39	(3,6,39)
(4,5,6,1)	2	100	192	(4,1,192)
(4,3,2)	1	50	45	(4,2,45)
(4,3)	1	187.5	181	(4,3,181)
(4,5)	1	87.5	81	(4,5,81)
(4,5,3,6)	2	62.5	114	(4,6,114)
(5,6,2,1)	1	37.5	32	(5,1,32)
(5,6,2)	1	100	98	(5,2,98)
(5,3)	1	125	122	(5,3,122)
(5,4)	1	162.5	153	(5,4,153)
(5,3,6)	1	50	45	(5,6,45)
(6,1)	1	150	124	(6,1,124)
(6,2)	1	100	88	(6,2,88)
(6,3)	1	50	46	(6,3,46)
(6,5,3,4)	1	12.5	12.5	(6,4,12.5)
(6,5)	1	112.5	88	(6,5,88)

served by new lightpath establishment and baseline lightpaths modulation adjustments if baseline lightpaths are not using highest-possible modulations.

Fig. 5(b) numerically depicts the performance on overall network throughput. Even without lightpath splitting, there is still room for an increase of network throughput. This improvement is possible as the baseline traffic is usually served with a certain amount of excess capacity (in both electrical and optical layers), and part of the spikes can be accepted by raising modulation levels of existing lightpaths, establishing new lightpaths using spare spectrum, and grooming onto existing lightpaths with spare electrical-layer bandwidth. Besides, we can also observe that *with lightpath splitting* can achieve similar performance as *all lightpath splitting*. The reason is that, during traffic fluctuations, some network links are under resource crunch, while some other links may still have spare capacity, this leads to the result that not all lightpaths need to be split. The results in Table III also support this point. The gap between *with lightpath splitting* and *all lightpath splitting* is due to the fact that the ILP did not finished its optimization within reasonable time (see footnote 8).

Fig. 5(c) shows the number of SplitPoints (number of added transceiver pairs) returned by the optimization model as traffic load increases. As expected, more SplitPoints are activated to accommodate incremental traffic spikes as load increases. Combining Figs. 5(b) and 5(c), an important message is that, by wisely selecting SplitPoints, lightpath splitting can achieve almost the same throughput as setting all intermediate nodes as SplitPoints (*all lightpath splitting*), while reducing the number of SplitPoints to mitigate impacts on existing traffic.

Table III shows the details of how SplitLightpaths are split into PostSplitLightpaths. We conclude that lightpaths with higher load tend to be selected as SplitLightpaths. As the load of traffic spike increases, more SplitLightpaths are involved.

C. Complexity Analysis

Table IV shows the problem size of the mathematical formulation. On time complexity, as our lightpath splitting problem involves lightpaths splitting decision and corresponding RMSA, as well as new lightpaths RMSA, it is more complex than classical RSA problems, which has been proved to be NP-hard [58]. Therefore, our problem is NP-hard.

V. SCALABLE ALGORITHMS FOR LIGHTPATH SPLITTING

The mathematical optimization can process all traffic requests and return the whole network configurations after lightpath splitting simultaneously, but it has high computational complexity. To design scalable algorithms, we follow the divide-and-conquer rule for quickly solving the problem.

For baseline traffic accommodation, we try to minimize number of used transceivers (the MinLP policy in [59]). The modulation level is assigned following the practical principle that highest-possible modulation level is used [60]. Traffic requests are served in descending order of requested bandwidth.

A. Divide-and-Conquer Problem Decomposition

Similar to designing a multi-layer optical network [61], the problem of lightpath splitting can be partitioned into the following subproblems (which are not necessarily independent):

1) Decide the Number of SplitPoints on Baseline Lightpaths: determine the number (K) of SplitPoints (also the number of added transceiver pairs) on baseline configurations.

TABLE III

OPTIMIZATION RESULTS: UNSPLITLIGHTPATHS, SPLITLIGHTPATHS, POSTSPLITLIGHTPATHS AND LIGHTPATH LOAD

UnsplitLightpaths*	Load (Gb/s)	Possible SplitLightpaths	Load (Gb/s)	PostSpliLightpaths**				
				$\mu=1$	$\mu=2$	$\mu=3$	$\mu=4$	$\mu=5$
(5,3,6)	45	(1,2,3,6)	195	(1,2,3,6)	**(1,2), (2,3,6)**	**(1,2), (2,3,6)**	**(1,2), (2,3), (3,6)**	**(1,2), (2,3), (3,6)**
(3,2,6)	39	(4,5,6,1)	192	(4,5,6,1)	**(4,5), (5,6,1)**	**(4,5), (5,6,1)**	**(4,5), (5,6), (6,1)**	**(4,5), (5,6), (6,1)**
(2,3,4)	37	(4,5,3,6)	114	(4,5,3,6)	**(4,5,3), (3,6)**	**(4,5), (5,3), (3,6)**	**(4,5), (5,3), (3,6)**	**(4,5), (5,3), (3,6)**
(2,6,5)	24	(1,6,3)	103	(1,6,3)	**(1,6), (6,3)**	**(1,6), (6,3)**	**(1,6), (6,3)**	**(1,6), (6,3)**
		(5,6,2)	98	(5,6,2)	(5,6,2)	**(5,6), (6,2)**	(5,6,2)	(5,6,2)
		(1,6,5)	71	(1,6,5)	(1,6,5)	**(1,6), (6,5)**	**(1,6), (6,5)**	**(1,6), (6,5)**
		(1,6,3,5,4)	47	(1,6,3,5,4)	(1,6,3,5,4)	**(1,6), (6,3,5,4)**	**(1,6), (6,3), (3,5), (5,4)**	**(1,6), (6,3,5), (5,4)**
		(4,3,2)	45	(4,3,2)	(4,3,2)	**(4,3), (3,2)**	**(4,3), (3,2)**	**(4,3), (3,2)**
		(3,2,1)	33	(3,2,1)	(3,2,1)	(3,2,1)	(3,2,1)	**(3,2), (2,1)**
		(5,6,2,1)	32	(5,6,2,1)	**(5,6,2), (2,1)**	**(5,6), (6,2,1)**	**(5,6), (6,2,1)**	**(5,6,2), (2,1)**
		(6,5,3,4)	12.5	(6,5,3,4)	(6,5,3,4)	**(6,5), (5,3), (3,4)**	(6,5,3,4)	**(6,5), (5,3), (3,4)**

* One-hop lightpaths that traverse no intermediate nodes on optical layer are not shown here. They also belong to the category of UnsplitLightpaths.
** For each μ, only bolder ones refer to PostSplitLightpaths, while normal ones are UnsplitLightpaths.

TABLE IV

SIZE OF FORMULATIONS FOR LIGHTPATH SPLITTING

Variables	$\mathcal{O}(\lvert\mathbf{L}\rvert\lvert\mathbf{N}\rvert^2\lvert\mathbf{E}\rvert F+\lvert\mathbf{L}\rvert\lvert\mathbf{N}\rvert^2\lvert\mathbf{A}\rvert+\lvert\mathbf{R}\rvert\lvert\mathbf{N}\rvert^2)$
Constraints	$\mathcal{O}(\lvert\mathbf{L}\rvert\lvert\mathbf{N}\rvert^2\lvert\mathbf{E}\rvert F+\lvert\mathbf{L}\rvert\lvert\mathbf{N}\rvert^2\lvert\mathbf{A}\rvert F+\lvert\mathbf{R}\rvert\lvert\mathbf{N}\rvert^2+\lvert\mathbf{N}\rvert^3)$

2) Which Lighpath and How to Split the Lightpath: determine which baseline lightpaths to be split, and how to split each lightpath.

3) PostSplitLightpaths Resource Allocation: remove SplitLightpaths and allocate spectrum to PostSplitLightpaths.

4) Incremental Traffic Routing After Lightpath Splitting: setup new lightpaths if necessary, and route incremental traffic on the network consisting of un-split baseline lightpaths, PostSplitLightpaths, and newly-setup lightpaths.

The heuristic cannot solve the four subproblems as a whole. So, we transform subproblem 1 into a decisive variable input, controlling how many lightpath-splitting operations are executed in network. When the number of SplitPoints, K, is set to be a controlled variable, subproblem 2 can be transformed into a simpler one, i.e., the *lightpath-SplitPoint-selection problem*, which is the goal for heuristic design. Subproblems 3, 4 act as post-split operations, which will be discussed in Section V.D.

Finally, the logical flow for using heuristic algorithms to solve the lightpath splitting problem is: 1) when traffic spikes first arrive, part of the spikes can be accepted by the network using spare capacities. 2) As this gap is filled up to compose an extended baseline network configuration, lightpath splitting is triggered. At this stage, we should first decide the number of SplitPoints. 3) Then, we should determine the distribution of these SplitPoints on the extended baseline network configuration, and how to allocate spectrum to the PostSplitLightpaths. 4) Finally, we route the rest of the traffic spikes on this network configuration by both grooming [59], [62] onto existing lightpaths, or setting up new lightpaths. To maximize network throughput, all traffic requests are served one by one following a descending order of requested bandwidth based on multi-layer auxiliary graphs [59], [63].

B. Pre-Splitting Preparations

When incremental traffic spikes arrive, we first use Algorithm 1 to accommodate as many requests as possible before lightpath splitting using spare capacity in both optical and electrical layers. This is also the normal operation for networks without lightpath splitting when traffic spikes arrive. Lightpath splitting is triggered when there is not enough capacity for serving more traffic. The network configuration at this time is the starting point for lightpath splitting.

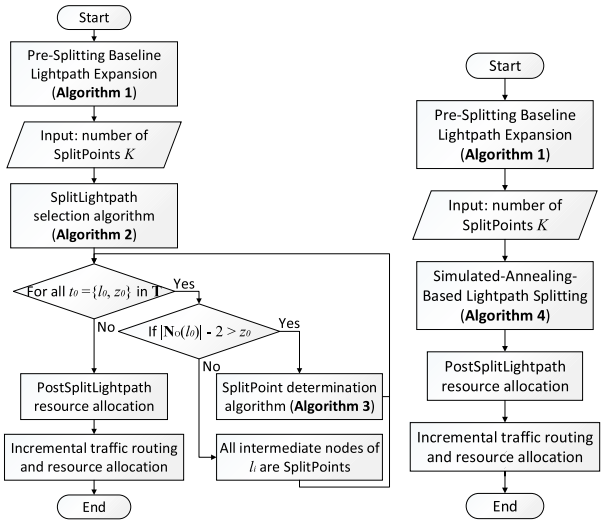

(a) Greedy lightpath splitting. (b) SA lightpath splitting.

Fig. 6. Flowchart for different lightpath-splitting algorithms.

C. Solving the Lightpath-SplitPoint-Selection Problem

Formally, given a network topology $\mathbf{G}(\mathbf{N},\mathbf{E})$, the *lightpath-SplitPoint-selection problem* is to find K SplitPoints on all existing lightpaths possible to be split. We try both greedy and Simulated-Anneal (SA) methods to solve the problem.

1) Greedy Lightpath Splitting: In greedy lightapth splitting algorithm, we concentrate on which lightpaths, i.e., SplitLightpaths, to split (solved by Algorithm 2: SplitLightpaths selection), and where to split along the lightpath (solved by Algorithm 3: SplitPoints determination). The execution flowchart of the two algorithms can be found in Fig. 6(a).

- *Which Lightpath to Split?*

According to Definition 1-3, we define a SplitLightpaths set $\mathbf{T}$ consisting of tuples: $t_i=[l_i,z_i]$, which represents that SplitLightpath l_i is to be split z_i times into z_i+1 PostSplitLightpaths by z_i SplitPoints $\mathbf{V}_{l_i}=\{[v_1,l_i],[v_2,l_i],\ldots,[v_{z_i},l_i]\}$, $v_1,v_2,\ldots,v_{z_i}\in\mathbf{N}_O(l_i)$.

Algorithm 1 Baseline Lightpath Expansion (also performs as *w/o Lightpath Splitting*)

Input: baseline network configurations with baseline lightpaths set $\mathbf{L}$; incremental traffic profile $\mathbf{R_I}$;
Output: expanded baseline lightpaths set $\mathbf{L_E}$; incremental traffic residual profile $\mathbf{R_{I,r}}$;
sort all incremental traffic $\tilde{r} \in \mathbf{R_I}$ in descending order of bandwidth $\tilde{b}_{\tilde{r}}$;
$\mathbf{L_E} \leftarrow \mathbf{L}$
for $i = 0$ to $|\mathbf{R_I}|$ **do**
  route $\tilde{r_i}$ with maximum bandwidth possible ($\tilde{b}_{\tilde{r},m}$) on baseline network configurations using multi-layer auxiliary graph model [63], and add the new lightpath into $\mathbf{L_E}$; the unserved bandwidth ($\tilde{b}_{\tilde{r}} - \tilde{b}_{\tilde{r},m}$) of each request forms $\mathbf{R_{I,r}}$;
end for

Basically, previous optimization results in Table III reveal that lightpaths under larger load tend to be split earlier. Then, we follow this thread to design Algorithm 2. Inspired by strategies of breadth-first or depth-first search algorithms, we introduce two greedy options to either set at least one SplitPoint per SplitLightpath so as to split as many lightpaths as possible (BF: Breath First), or set as many SplitPoints as possible on the SplitLightpaths to split lightpaths harder (DF: Depth First).[9]

- *How to Split the selected SplitLightpaths?*

When Algorithm 2 returns the SplitLightpaths set $\mathbf{T}$, we further apply Algorithm 3 to determine the exact SplitPoints on SplitLightpaths. In Algorithm 3, we further evaluation two greedy options: either to maximize electrical-layer capacity by adjusting modulation level without shrinking occupied spectrum (MaxE), or to maximize optical-layer available resources by adjusting modulation level while shrinking occupied spectrum (MaxO), as first introduced in Section III.A.

Finally, by combining the two policies on which lightpath to split and the two policies on how to split the selected SplitLightpaths, we introduce four policies for greedy lightpath splitting: BF-MaxE, DF-MaxE, BF-MaxO, and DF-MaxO.

2) Simulated-Annealing (SA)-Based Lightpath Splitting: In this section, we define a basic operation, *SplitPoint exchange* (inspired by node-exchange [61] and branch-exchange [64]), for designing a lightpath-splitting algorithm based on SA.

*Definition 4: In a **SplitPoint-exchange** operation, a SplitPoint inside the candidate set is swapped with other SplitPoint outside the candidate set. Mathematically, there is a set* $\mathbf{V}$ *comprises all possible SplitPoints (represented by* $V_i = [v, l]$*). Then, we have a candidate SplitPoint set* $\mathbf{V_c}$ *with* $|\mathbf{V_c}| = K$ *elements,* $\mathbf{V_c} \subseteq \mathbf{V}$*. Randomly select* $\forall V_i \in \mathbf{V_c}, V_j \in \mathbf{V} \setminus \mathbf{V_c}$*, delete* V_i *from* $\mathbf{V_c}$*, while put* V_j *into* $\mathbf{V_c}$ *to form a new* $\mathbf{V_c}'$*.*

For such a SplitPoint exchange, neighboring configurations $\mathbf{V_c}'$ that returns better results (higher network throughput Y) than original configurations (baseline network throughput Y_0) $\mathbf{V_c}$ will be accepted. Meanwhile, those whose outputs after the SplitPoint-exchange operation are worse than the initial state

[9]It should be noted that, as K grows larger, BF and DF policies will finally converge with *all lightpath splitting* policy, as all possible intermediate nodes are selected as SplitPoints.

Algorithm 2 Greedy SplitLightpaths Selection

Input: number of SplitPoints K; expanded baseline lightpaths set $\mathbf{L_E}$; incremental traffic residual profile $\mathbf{R_{I,r}}$; *greedy options*: breadth first ($g_1 = 0$) or depth first ($g_1 = 1$);
Output: SplitLightpaths set $\mathbf{T}$;
construct a virtual topology $\mathbf{G}'(\mathbf{N}, \mathbf{L_E} \cup \mathbf{E})$ consisting of $\mathbf{N}$ nodes, and lightpaths in $\mathbf{L_E}$ as edges with infinite capacity, and available optical resources as edges with actual optical capacity;
for $j = 1$ to $|\mathbf{R_{I,r}}|$ **do**
  route residual bandwidth of $\tilde{r_j}$ on $\mathbf{G}'$;
end for
sort lightpath $l_i \in \mathbf{L_E}$ in descending order of bandwidth;
if $g_1 = 0$ **then**
  for $k = 1$ to K **do**
    if $|\mathbf{N}_O(l_k)| > 2$ **then**
      add $[l_k, 1]$ into $\mathbf{T}$;
    end if
  end for
  if $|\mathbf{T}| < K$ **then**
    $t \leftarrow 1$;
    while $t < K - |\mathbf{T}|$ **do**
      if $|\mathbf{N}_O(l_k)| - 2 > K - |\mathbf{T}| - t$ **then**
        revise $[l_t, 1]$ to be $[l_t, K - |\mathbf{T}| - t]$;
        $t \leftarrow K - |\mathbf{T}|$;
      else
        revise $[l_t, 1]$ to be $[l_t, |\mathbf{N}_O(l_k)| - 2]$;
        $t \leftarrow t + |\mathbf{N}_O(l_k)| - 2$;
      end if
    end while
  end if
else
  $k \leftarrow 1$;
  while $k < K$ **do**
    if $|\mathbf{N}_O(l_k)| - 2 > K - k$ **then**
      add $[l_k, K - k]$ into $\mathbf{T}$;
      $k \leftarrow K$;
    else
      add $[l_k, |\mathbf{N}_O(l_k)| - 2]$ into $\mathbf{T}$;
      $k \leftarrow k + |\mathbf{N}_O(l_k)| - 2$;
    end if
  end while
end if

are accepted with a variable acceptance probability ϑ lying on the "system temperature" τ, which is gradually decreasing as the algorithm progresses to simulate the annealing process. The algorithm will terminate when τ reaches the "ending temperature" τ_e, and returns results, where:

$$\vartheta = \begin{cases} 1, & Y \geq Y_0 \\ \exp(-\dfrac{Y_0 - Y}{\tau}), & Y < Y_0 \end{cases} \tag{36}$$

The SA-based lightpath splitting (algorithm 4) method can return the SplitPoint set $\mathbf{V}$ directly. However, the remaining unsolved problem is how to allocate spectrum for PostSplitLightpaths. Then, we combine the previously dis-

Algorithm 3 Greedy SplitPoints Determination

Input: a SplitLightpath $t_0 = [l_0, z_0]$, number of occupied spectrum slots $W(l_0)$, and modulation level $S(l_0)$; *greedy options*: MaxE ($g_2 = 0$) or MaxO ($g_2 = 1$);
Output: SplitPoint set $\mathbf{V}(l_0) = \{[v_1, l_0], [v_2, l_0], \ldots, [v_{z_0}, l_0]\}$ for SplitLightpaths $t_0 = [l_0, z_0]$;
1: sum of electrical-layer capacity $Q \leftarrow 0$; sum of occupied spectrum slots $U \leftarrow \infty$;
2: **for** all possible $\{v_1, v_2, \ldots, v_{z_0}\} \subsetneqq \mathbf{N}_O(l)$ **do**
3: lightpath l_0 is split into z_0+1 segments: $l_1, l_2, \ldots, l_{z_0+1}$;
4: raise $S(l_1)$, $S(l_2)$, ..., $S(l_{z_0+1})$ to the maximum possible;
5: **if** $g_2 = 0$ **then**
6: $Q_i \leftarrow \sum_{1 \le k \le z_0+1} W(l_k) S(l_k)$;
7: **if** $Q_i > Q$ **then**
8: $\mathbf{V}(l_0) \leftarrow \{[v_1, l_0], [v_2, l_0], \ldots, [v_{z_0}, l_0]\}$;
9: **end if**
10: **else**
11: shrink $W(l_1^i)$, $W(l_2^i)$, ..., $W(l_{z_0}^i)$ to the minimum possible;
12: $U_i \leftarrow \sum_{1 \le k \le z_0+1} W(l_k)$;
13: **if** $U_i < U$ **then**
14: $\mathbf{V}(l_0) \leftarrow \{[v_1, l_0], [v_2, l_0], \ldots, [v_{z_0}, l_0]\}$;
15: **end if**
16: **end if**
17: **end for**

Algorithm 4 SA-Based Lightpath Splitting

Input: number of SplitPoints K; expanded baseline lightpaths set $\mathbf{L_E}$; incremental traffic residual profile $\mathbf{R_{I,r}}$; SA initial temperature τ_0, ending temperature τ_e, and cooling parameter γ;
Output: SplitPoint set $\mathbf{V} = \{\mathbf{V}_{l_0}, \mathbf{V}_{l_1}, \ldots, \mathbf{V}_{l_n}\}$
1: $\tau \leftarrow \tau_0$;
2: randomly select K SplitPoints, and put them into $\mathbf{V_c}$;
3: lightpath splitting resource allocation; incremental traffic routing and resource allocation; Y_0 $\leftarrow$current network throughput;
4: **while** $\tau > \tau_e$ **do**
5: randomly select $V_i \in \mathbf{V_c}, V_j \in \mathbf{V} \setminus \mathbf{V_c}$, and perform SplitPoint exchange;
6: lightpath splitting resource allocation; incremental traffic routing and resource allocation; Y $\leftarrow$current network throughput;
7: **if** $\vartheta >$ random(0,1) **then**
8: delete V_i from $\mathbf{V_c}$, put V_j into $\mathbf{V_c}$ to form a new $\mathbf{V_c}'$;
9: **end if**
10: cooling the annealing temperature $\tau \leftarrow \tau \cdot \gamma$;
11: **end while**

cussed policies (MaxE and MaxO) with SA, and introduce two policies: SA-MaxE and SA-MaxO.

D. Post-Splitting Configurations

As shown in Fig. 6, post-splitting network configurations, i.e., lightpath splitting resource allocation and incremental traffic accommodation, should be executed after deciding which and how to split lightpaths. For MaxE policies, spectrum allocation is not changed. For MaxO policies, we use a First-Fit strategy to reassign shrunken spectrum slots with smaller index to reduce spectrum fragmentation. On incremental traffic accommodation, we still use the multi-layer auxiliary graph network model as of baseline traffic [59], [63].

E. Complexity Analysis

1) Greedy Lightpath Splitting: Greedy lightpath splitting scheme first determines SplitLightpaths (Algorithm 2) with the complexity of $\mathcal{O}(|\mathbf{R_{I,r}}||\mathbf{N}|^2 + |\mathbf{L_E}|^2 + K)$. Then, there is a loop for executing Algorithm 3 to split each lightpaths in $\mathbf{T}$. In Algorithm 3, for each SplitLightpath $t_0 = [l_0, z_0]$, there are $\binom{|\mathbf{N}_O(l_0)|-2}{z_0}$ possible $\{v_1, v_2, \ldots, v_{z_0}\}$ from $\mathbf{N}_O(l_0)$, based on principles of combinatorial number. In lightpath splitting resource allocation, at most $2K$ PostSplitLightpaths will use first fit to try at most F slots to reallocate spectrum resource, resulting in a complexity of $\mathcal{O}(KF)$. While in incremental traffic accommodation, the size of auxiliary graph is $(F + 1)|\mathbf{N}|$ [63]. The complexity of running Dijkstra for RMSA is $\mathcal{O}(|\mathbf{N}|^2 F^2)$. So, the total complexity is $\mathcal{O}(|\mathbf{R_{I,r}}||\mathbf{N}|^2 + |\mathbf{L_E}|^2 + K) + \mathcal{O}(|\mathbf{T}|\binom{|\mathbf{N}_O(l_0)|-2}{z_0}) + \mathcal{O}(KF) + \mathcal{O}(|\mathbf{N}|^2\ F^2)$.

As the number of SplitLightpaths is no larger than the number of SplitPoints, $|\mathbf{T}| \le K$. The number of incremental traffic residual requests between node pairs should be no larger than the square of node number, $|\mathbf{R_{I,r}}| \le |\mathbf{N}|^2$. The number of expanded baseline lightpaths should be no larger than the number of spectrum slots times the square of node number, $|\mathbf{L_E}| \le F|\mathbf{N}|^2$. For BF policies, $z_0 = 1$, $\binom{|\mathbf{N}_O(l_0)|-2}{1} = |\mathbf{N}_O(l_0)| - 2 < |\mathbf{N}|$. For DF policies, $z_0 = |\mathbf{N}_O(l_0)| - 2$ is true in most lightpaths, $\binom{|\mathbf{N}_O(l_0)|-2}{|\mathbf{N}_O(l_0)|-2} = 1$. While there is only one possible lightpath that $1 \le z_0 \le |\mathbf{N}_O(l_0)| - 2$. The number of nodes a lightpath traverses should be no larger than the total number of nodes, so, $\binom{|\mathbf{N}_O(l_0)|-2}{z_0} < \binom{|\mathbf{N}|}{z_0} \sim |\mathbf{N}|^{z_0}$. The final complexity is $\mathcal{O}(F^2|\mathbf{N}|^4 + K|\mathbf{N}|^{z_0} + KF)$.

2) SA-Based Lightpath Splitting: The complexity of SA is related to SA initial temperature τ_0, ending temperature τ_e, and cooling parameter γ. In our algorithm, there is a loop controlled by current temperature τ. The execution times κ of this loop can be determined as follows:

$$\tau_0 \cdot \gamma^{\kappa-1} > \tau_e > \tau_0 \cdot \gamma^{\kappa} \tag{37}$$

On each τ, a SplitPoint-exchange operation and current throughput calculation are performed. As analyzed before, the complexity of lightpath splitting resource allocation and incremental traffic accommodation is $\mathcal{O}(F^2|\mathbf{N}|^2)$. The final complexity is $\mathcal{O}(\kappa F^2|\mathbf{N}|^2)$.

VI. Illustrative Numerical Examples

A. Simulation Setup

In this section, we implement the proposed algorithms by a network simulator developed on C++ to evaluate the performance of lightpath splitting. We use NSFNET backbone topology (modified to avoid crosslinks, Fig. 7). All fibers are unidirectional with 30 spectrum slots, and the spectrum width of each slot is 12.5 GHz. Each node is equipped with enough transceivers for lightpath splitting as we analyzed before in Assumption 1. For each simulation run, the traffic

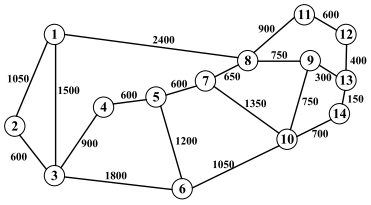

Fig. 7. NSFNET network topology (14 nodes, 20 bidirectional links).

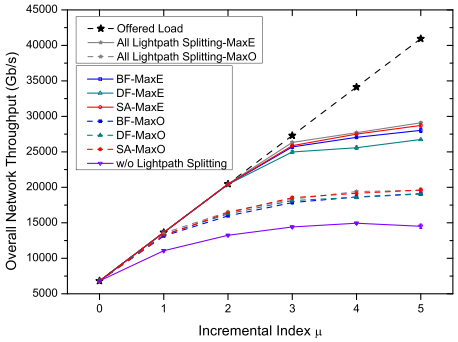

Fig. 8. Overall network throughput vs. μ, when $K = 150$.

bandwidth between any node pair is randomly decided obeying a uniform distribution in the open interval (0, 75) Gb/s with 6.25 Gb/s granularity. For fairness among different simulation runs, the overall requested baseline bandwidth is fixed to be the average total bandwidth: $\frac{0+75}{2} \cdot |\mathbf{N}| \cdot (|\mathbf{N}| - 1)$ Gb/s. Incremental index μ, as defined before, controls the severity of traffic spikes.

In SA, initial temperature $\tau_0 = 100 \cdot e^{K/10}$, ending temperature $\tau_e = 0.01/K^3$, and cooling parameter $\gamma = 0.95$. The results shown are acquired from the average performance of 40 parallel simulations and results are plotted with confidence intervals at 95% confidence level.

B. How Much Do We Gain?

Figs. 8-10 provide answers for how much throughput increase can we gain via different lightpath-splitting methods under different network settings. We see that MaxE policies always outperform MaxO policies, because they increase the capacity in different ways. MaxE maps the increased capacity in electrical layer, while MaxO puts the resource in optical layer. However, electrical-layer resources are more flexible to be used than optical-layer resources, which is enforced by spectrum continuity and contiguity constraints. We also find that, in most cases, SA policies outperform BF and DF policies, as expected, as SA can avoid local optima.

Fig. 8 presents relationship between overall network throughput (baseline and incremental traffic) and incremental index μ when the number of SplitPoints (also the number of added transceiver pairs) K is 150. This figure presents a similar result as in Fig. 5(b) of network optimization results. We find that lightpath splitting policies can significantly increase network throughput with respect to *w/o lightpath splitting* whose throughput curve goes to flat at 15000 Gb/s. Besides, when incremental traffic is not so severe ($\mu \in [0, 2]$), MaxE policies can provide as much throughput as the offered load (no traffic blocking). As μ continues to be larger, MaxE policies (especially SA-MaxE) perform almost the same as

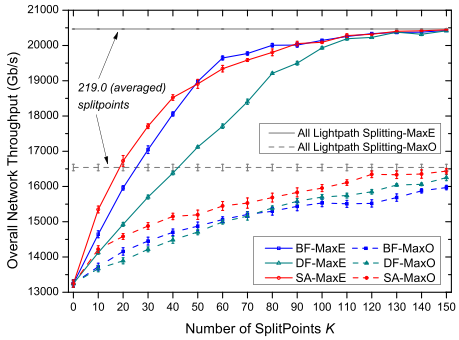

Fig. 9. Overall network throughput vs. K, when $\mu = 2$.

all lightpah splitting (25000-30000 Gb/s, almost double the throughput of *w/o lightpath splitting*).

When we fix μ to be 2, and observe how overall network throughput performs in different number of K, we get Fig. 9. For a given amount of incremental traffic, e.g., $\mu = 2$, higher overall throughput can be gained as K becomes larger. It can be noticed that, when K grows to be 140 or 150, the throughput performance is almost the same as *all lightpath splitting*, whose K is around 219.0. This result reveals that a proper selection of SplitPoints is crucial for lightpath splitting.

For further understanding the relationships among throughput, K, and μ, we plot Fig. 10, separating MaxE and MaxO results in two subfigures for readability. Here, we use normalized incremental throughput (with respect to the amount of incremental traffic) to fairly evaluate how much incremental traffic is served under different K and μ. We find common trends, that in MaxE policies, BF performs better than DF. This is due to the fact that BF policies can involve more lightpaths into lightpath splitting without changing spectrum occupancy, resulting in more capacity on electrical layer. In MaxO policies, there is a crossing point that, when K is small, BF achieves better than DF, while DF gradually outperforms BF as the number of K increases. This is due to different lightpath spectrum reallocation results in BF and DF policies. In MaxO policies, splitting a lightpath harder (DF) may provide more available spectrum when the number of SplitLightpaths becomes larger as K increases.

C. How Much Do We Compromise?

Fig. 11(a) presents the relationship between normalized affected traffic amount (with respect to the amount of traffic after Algorithm 1, when lightpath splitting is going to be triggered) vs. K when $\mu = 2$. For *all lightpath splitting* policies, there is around 54% traffic affected, the remaining 46% are those carried by one-hop lightpaths which cannot be split. We find that BF policies generally affect more traffic than SA and DF methods, while DF methods affect the least. This phenomenon is easy to understand because BF policies prefer to use as many lightpaths as possible, thus affecting more traffic, while DF policies tend to split lightpaths harder and involve the least number of lightpaths. For BF policies when K reaches 130 or larger, though they activate much less SplitPoints than *all lightpath splitting* (219.0 SplitPoints on average), the amount of affected traffic is the same. This discovery tells us that fewer SplitPoints does not necessarily mean less affected traffic. Once again it shows that a smart selection

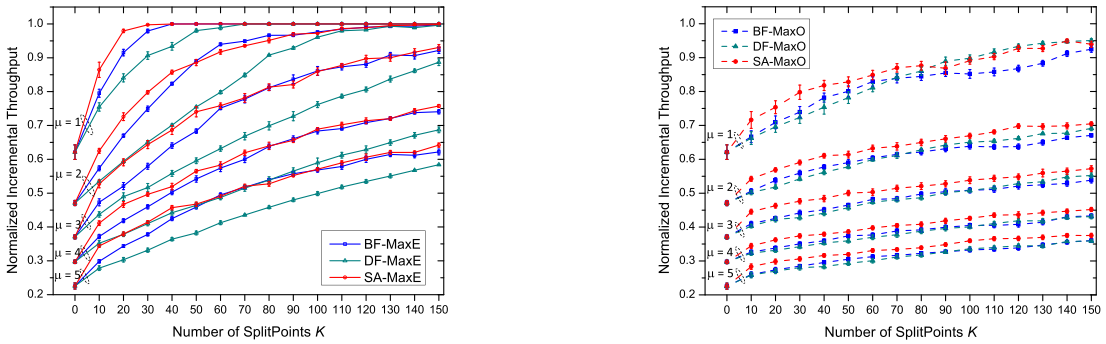

(a) MaxE polocies. (b) MaxO policies.

Fig. 10. Normalized incremental throughput (with respect to the amount of incremental traffic) vs. number of SplitPoints vs. incremental index μ.

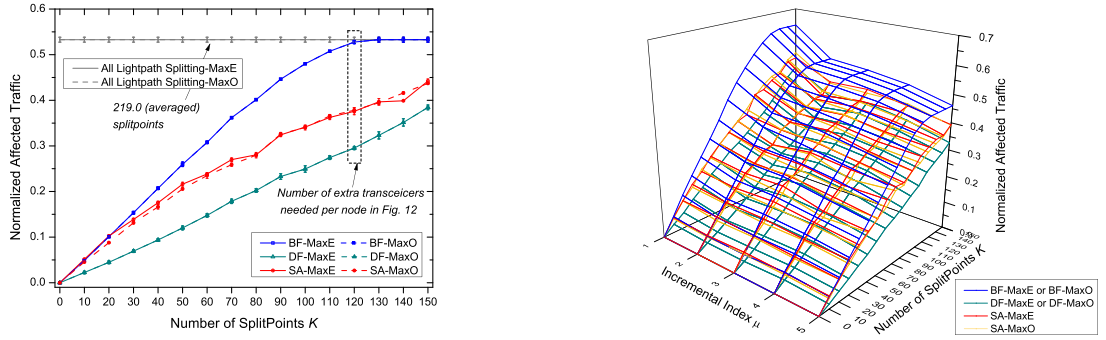

(a) Normalized affected traffic vs. K, when $\mu = 2$. (b) Normalized affected traffic vs. K vs. μ.

Fig. 11. Normalized affected traffic (with respect to the amount of supporting traffic after Algorithm 1).

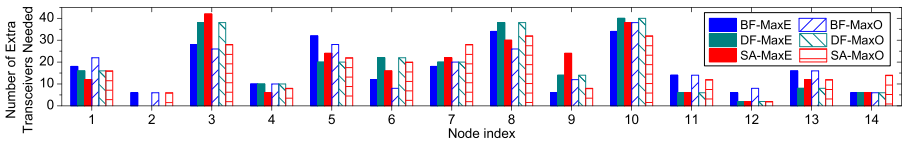

Fig. 12. The number of extra transceivers needed in each node, when $\mu = 2$ and $K = 120$.

of SplitPoints is crucial from the perspective of affected traffic. Fig. 11(b) depicts the relationship among normalized affected traffic vs. K in different μ. We find similar trends as in Fig. 11(a). Then, the conclusion drawn from Fig. 11(a) can be generalized to other situations with different μ.

Fig. 12 shows how many extra transceivers are needed for each node of the network in a simulation run, when $\mu = 2$ and $K = 120$ (as discussed in Section III.E, the total number of increased transceivers is equal to twice the number of K). We find that higher-degree nodes in the topology tend to need more additional transceivers during lightpath splitting.

In Fig. 13, we study how average traffic hops performs as K increases when $\mu = 2$. Here, we define average traffic hops per b/s to evaluate the average hops per unit bandwidth of all traffic on electrical layer. Multiple hops on electrical layer means multiple electrical processing, possibly resulting in higher end-to-end latency and energy consumption. We observe from Fig. 13 that MaxE policies result in larger traffic hops than MaxO, due to the fact that MaxO policies keep resources in the optical layer and leave more opportunities for setting up lightpaths to directly support traffic without intermediate nodes in electrical layer. Also, DF policies result in more traffic hops when K is larger (more than 40), and this is because DF policies tend to split lightpaths more aggressively.

Besides, the increased energy consumption is mainly caused by the increased number of transceivers, which is directly proportional to the number of K shown in almost all figures.

D. Trade-Off Curve by Pareto Front Analysis

As analyzed before, both logically in Section III and numerically in Section VI.B and VI.C, lightpath splitting can gain throughput increase with compromise of affecting existing traffic. What is the exact relationship between these two interacting user-experience-coupled variables? This answer is important for the network operator to choose a proper way to apply lightpath splitting.

In Fig. 14, we plot the Pareto front on throughput gained and traffic affected by lightpath splitting when $\mu = 2$. As expected, higher throughput is achieved at the cost of less unaffected traffic. A clear message from the figure is that *all lightpath splitting* is not an economical choice, as our proposed lightpath-splitting policies (both DF and SA for either MaxE or MaxO) can achieve similar throughput with much more unaffected traffic. We also learn from the figure that BF is not as efficient as DF and SA, because it always affects more traffic for a network throughput value. It is worth pointing out that, if we expect lightpath-splitting policies to return the highest throughput possible, BF policies are even worse than

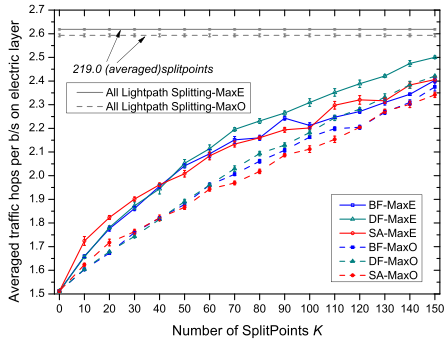

Fig. 13. Average traffic hops per b/s on electrical layer vs. K, when $\mu = 2$.

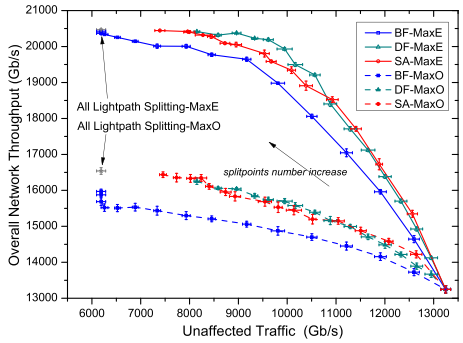

Fig. 14. Pareto front of throughput vs. unaffected traffic, when $\mu = 2$.

TABLE V
ELAPSED RUNNING TIME (SECONDS) WHEN $\mu = 2$

K	BF		DF		SA	
	MaxE	MaxO	MaxE	MaxO	MaxE	MaxO
10	1.096	1.229	1.209	1.240	337.390	374.280
80	0.176	0.940	0.355	0.956	137.635	545.693
150	0.109	0.823	0.117	0.808	63.593	611.494

all lightpath splitting, as BF policies achieve less throughput while affecting the same amount of traffic. There is a small upturned tail when the unaffected traffic is becoming small for BF policies. This is because BF policy has involved all lightpaths in lightpath splitting, and further lightpath splitting operations will be executed on those lightpaths that already have at least one SplitPoints.

Another observation that should be discussed is the slope of the Pareto-front curve. This slope can be regarded as the ratio of "gain" to "sacrifice", describing the marginal utility of yield provided by lightpath splitting. When lightpath splitting is triggered, as K increases (from lower right to upper left on the figure), the slope is gradually diminishing to almost zero. This phenomenon teaches us that the first few SplitPoints with careful selection can gain more throughput increase than affected traffic; however, as the number of SplitPoints grows, the marginal utility of throughput increase diminishes. From the operators' point of view, the incentive for introducing too many SplitPoints is weak. Therefore, a proper selection of the first few SplitPoints is critical. By using our proposed methods, the operator can address this problem proactively.

It should be highlighted that points on this Pareto-front curve represent the performance boundary for different lightpath-splitting policies. Moving along the curve by different points can provide the network operator various options to obtain throughput gains by affecting a fraction of existing traffic using lightpath splitting. For different network topologies, spectrum resources, and traffic profiles, the exact location of the curve may vary with situations, but its trend of diminishing marginal throughput increase is general to other network instances.

E. Execution Efficiency of the Proposed Algorithms

From Table V, we find that the execution time for greedy algorithms is on the order of several seconds, while SA-based algorithms take longer time (several minutes) because they need multiple iterations. Generally, the short-term traffic spikes studied in this paper last several hours or days, because they are caused by mega events as discussed in Section I. Therefore, the computational time of our proposed algorithms is acceptable to deal with short-term traffic spikes.

VII. CONCLUSION

In this study, we proposed a novel network reconfiguration scheme with lightpath splitting to provision short-term traffic fluctuations. Lightpath splitting was first introduced to provide more elasticity for incremental traffic spikes. We mathematically formulated the lightpath splitting problem, and solved the optimization model in a small network example. We further devised scalable heuristic algorithms for lightpath splitting in practical networks. Simulation results showed that, by wisely selecting SplitPoints, we can achieve higher throughput gains for incremental traffic spikes with as little affected traffic as possible. A Pareto front for different lightpath-splitting policies was presented for the network operator to choose proper network configurations when facing traffic spikes.

ACKNOWLEDGMENT

The authors would like to acknowledge P. J. Winzer, A. Cai, and Y. Li for enlightening discussions.

REFERENCES

[1] M. Gerla and L. Kleinrock, "On the topological design of distributed computer networks," *IEEE Trans. Commun.*, vol. COMM-25, no. 1, pp. 48–60, Jan. 1977.
[2] C.-Y. Hong *et al.*, "Achieving high utilization with software-driven WAN," *ACM SIGCOMM Comput. Commun. Rev.*, vol. 43, no. 4, pp. 15–26, Aug. 2013.
[3] G. Rizzelli, A. Morea, M. Tornatore, and O. Rival, "Energy efficient Traffic-Aware design of on–off multi-layer translucent optical networks," *Comput. Netw.*, vol. 56, no. 10, pp. 2443–2455, Jul. 2012.
[4] Y. Lui, G. Shen, and W. Shao, "Design for energy-efficient IP over WDM networks with joint lightpath bypass and router-card sleeping strategies," *IEEE/OSA J. Opt. Commun. Netw.*, vol. 5, no. 11, pp. 1122–1138, Nov. 2013.
[5] A. Morea, J. Perello, and S. Spadaro, "Traffic variation-aware networking for energy efficient optical communications," in *Proc. ONDM*, Apr. 2013, pp. 29–34.
[6] A. Morea, O. Rival, N. Brochier, and E. Le Rouzic, "Datarate adaptation for night-time energy savings in core networks," *J. Lightw. Technol.*, vol. 31, no. 5, pp. 779–785, Mar. 1, 2013.
[7] L. Stone. (2016). *Bringing Pokmon GO to Life on Google Cloud, Google Cloud Platform Blog*. https://cloudplatform.googleblog.com/2016/09/bringing-Pokemon-GO-to-life-on-Google-Cloud.html
[8] Akamai. (2015). *Black Friday Traffic Spikes 109 Percent Over Average Pre-Holiday Activity*. [Online]. Available: https://blogs.akamai.com/2015/12/2015-black-friday-traffic-spikes-109-percent-over-average-pre-holiday-activity.html
[9] J. Ryburn. (2017). *Black Friday vs. Cyber Monday: Traffic Insights from Kentik*. [Online]. Available: https://www.kentik.com/black-friday-vs-cyber-monday-traffic-insights-from-kentik/
[10] (2016). *Boosting International Backbone Capacity for Global Events Such as the RIO 2016 Olympics* [Online]. Available: http://us.ntt.net/news/viewFile.cfm/Capacity%20Magazine%20Aug%20Sept%202016%20NTT.pdf?file_id=200

[11] L. Chiaraviglio *et al.*, "Is green networking beneficial in terms of device lifetime?" *IEEE Commun. Mag.*, vol. 53, no. 5, pp. 232–240, May 2015.

[12] L. Chiaraviglio *et al.*, "Lifetime-aware ISP networks: Optimal formulation and solutions," *IEEE/ACM Trans. Netw.*, vol. 25, no. 3, pp. 1924–1937, Jun. 2017.

[13] J. Li, Z. Zhong, N. Hua, X. Zheng, and B. Zhou, "Balancing energy efficiency and device lifetime in TWDM-PON under traffic fluctuations," *IEEE Commun. Lett.*, vol. 21, no. 9, pp. 1981–1984, Sep. 2017.

[14] A. P. Vela, M. Ruiz, and L. Velasco, "Distributing data analytics for efficient multiple traffic anomalies detection," *Comput. Commun.*, vol. 107, pp. 1–12, Jul. 2017.

[15] L. Velasco *et al.*, "On-demand incremental capacity planning in optical transport networks," *IEEE/OSA J. Opt. Commun. Netw.*, vol. 8, no. 1, pp. 11–22, Jan. 2016.

[16] L. Velasco, A. P. Vela, F. Morales, and M. Ruiz, "Designing, operating, and reoptimizing elastic optical networks," *J. Lightw. Technol.*, vol. 35, no. 3, pp. 513–526, Feb. 1, 2017.

[17] D. Li, Y. Yu, J. Shi, and B. Zhang, "PALS: Saving network power with low overhead to ISPs and applications," *IEEE/ACM Trans. Netw.*, vol. 24, no. 5, pp. 2913–2925, Oct. 2016.

[18] T. Hashiguchi, K. Tajima, Y. Takita, and T. Katagiri, "Techniques for agile network re-optimization following traffic fluctuations," in *Proc. OFC*, Mar. 2017, pp. 1–3.

[19] E. Bouillet, J. F. Labourdette, R. Ramamurthy, and S. Chaudhuri, "Lightpath re-optimization in mesh optical networks," *IEEE/ACM Trans. Netw.*, vol. 13, no. 2, pp. 437–447, Apr. 2005.

[20] F. Solano, "Analyzing two conflicting objectives of the WDM lightpath reconfiguration problem," in *Proc. IEEE GLOBECOM*, Nov./Dec. 2009, pp. 1–7.

[21] F. Solano and M. Pióro, "Lightpath reconfiguration in WDM networks," *IEEE/OSA J. Opt. Commun. Netw.*, vol. 2, no. 12, pp. 1010–1021, Dec. 2010.

[22] Z. Zhong *et al.*, "Energy efficiency and blocking reduction for tidal traffic via stateful grooming in IP-over-optical networks," *IEEE/OSA J. Opt. Commun. Netw.*, vol. 8, no. 3, pp. 175–189, Mar. 2016.

[23] O. Gerstel, P. Lin, and G. Sasaki, "Wavelength assignment in a WDM ring to minimize cost of embedded SONET rings," in *Proc. IEEE INFOCOM*, Mar./Apr. 1998.

[24] G. Mohan, P. H. H. Ernest, and V. Bharadwaj, "Virtual topology reconfiguration in IP/WDM optical ring networks," *Comput. Commun.*, vol. 26, no. 2, pp. 91–102, Feb. 2003.

[25] N. Hua, H. Buchta, X. Zheng, H. Zhang, and B. Zhou, "Performance analysis of an improved postponed lightpath teardown strategy in multi-layer optical networks," in *Proc. ACP*, Nov. 2009, pp. 1–6.

[26] A. Bocoi *et al.*, "Reach-dependent capacity in optical networks enabled by OFDM," in *Proc. OFC*, Mar. 2009, pp. 1–3.

[27] T. Takagi *et al.*, "Dynamic routing and frequency slot assignment for elastic optical path networks that adopt distance adaptive modulation," in *Proc. OFC*, Mar. 2011, pp. 1–3.

[28] T. Tanaka, T. Inui, A. Kadohata, W. Imajuku, and A. Hirano, "Multi-period IP-over-elastic network reconfiguration with adaptive bandwidth resizing and modulation," *IEEE/OSA J. Opt. Commun. Netw.*, vol. 8, no. 7, pp. A180–A190, Jul. 2016.

[29] G. Huang, Y. Miyoshi, A. Maruta, Y. Yoshida, and K. Kitayama, "All-optical OOK to 16-QAM modulation format conversion employing nonlinear optical loop mirror," *J. Lightw. Technol.*, vol. 30, no. 9, pp. 1342–1350, May 1, 2012.

[30] R. Singh, M. Ghobadi, K. T. Foerster, M. Filer, and P. Gill, "Run, walk, crawl: Towards dynamic link capacities," in *Proc. ACM Workshop Hot Topics Netw.*, Nov. 2017, pp. 143–149.

[31] R. Singh, M. Ghobadi, K. T. Foerster, M. Filer, and P. Gill, "RADWAN: Rate adaptive wide area network," in *Proc. SIGCOMM*, Aug. 2018, pp. 547–560.

[32] S. S. Savas, M. F. Habib, M. Tornatore, F. Dikbiyik, and B. Mukherjee, "Network adaptability to disaster disruptions by exploiting degraded-service tolerance," *IEEE Commun. Mag.*, vol. 52, no. 12, pp. 58–65, Dec. 2014.

[33] C. S. K. Vadrevu, R. Wang, M. Tornatore, C. U. Martel, and B. Mukherjee, "Degraded service provisioning in mixed-line-rate WDM backbone networks using multipath routing," *IEEE/ACM Trans. Netw.*, vol. 22, no. 3, pp. 840–849, Jun. 2014.

[34] W. Hou, Y. Zong, X. Zhang, and L. Guo, "Adaptive service degradation in converged optical and data center networks," in *Proc. ACP*, Nov. 2014, pp. 1–3.

[35] M. Wang, M. Furdek, P. Monti, and L. Wosinska, "Restoration with service degradation and relocation in optical cloud networks," in *Proc. ACP*, Nov. 2015, p. 3, Paper ASu5F-2.

[36] R. B. R. Lourenço, M. Tornatore, C. U. Martel, and B. Mukherjee, "Running the network harder: Connection provisioning under resource crunch," *IEEE Trans. Netw. Service Manage.*, vol. 15, no. 4, pp. 1615–1629, Dec. 2018.

[37] Z. Zhong *et al.*, "On QoS-assured degraded provisioning in service-differentiated multi-layer elastic optical networks," in *Proc. IEEE GLOBECOM*, Dec. 2016, pp. 1–5.

[38] K. Christodoulopoulos, I. Tomkos, and E. A. Varvarigos, "Elastic bandwidth allocation in flexible OFDM-based optical networks," *J. Lightw. Technol.*, vol. 29, no. 9, pp. 1354–1366, May 1, 2011.

[39] J. Zhao, S. Subramaniam, and M. Brandt-Pearce, "Virtual topology mapping in elastic optical networks," in *Proc. IEEE ICC*, 2013, pp. 3904–3908.

[40] P. Chimento and J. Ishac, *Defining Network Capacity*, document IETF RFC 5136, 2008.

[41] Y. Li and D. C. Kilper, "Optical physical layer SDN," *IEEE/OSA J. Opt. Commun. Netw.*, vol. 10, no. 1, pp. A110–A121, Jan. 2018.

[42] D. C. Kilper, C. A. White, and S. Chandrasekhar, "Control of channel power instabilities in constant-gain amplified transparent networks using scalable mesh scheduling," *J. Lightw. Technol.*, vol. 26, no. 1, pp. 108–113, Jan. 1, 2008.

[43] F. Smyth, D. C. Kilper, S. Chandrasekhar, and L. P. Barry,, "Applied constant gain amplification in circulating loop experiments," *J. Lightw. Technol.*, vol. 27, no. 21, pp. 4686–4696, 2009.

[44] D. C. Kilper, M. Bhopalwala, H. Rastegarfar, and W. Mo, "Optical power dynamics in wavelength layer software defined networking," in *Proc. Photonic Netw. Devices*, Jan. 2015, p. 3, Paper NeT2F.2.

[45] P. J. Lin, "Reducing optical power variation in amplified optical network," in *Proc. Int. Conf. Commun. Technol.*, Apr. 2003, pp. 42–47.

[46] D. A. Mongardien, S. Borne, C. Martinelli, C. Simonneau, and D. Bayart, "Managing channels add/drop in flexible networks based on hybrid Raman/erbium amplified spans," in *Proc. ECOC*, Sep. 2006, pp. 1–2.

[47] A. S. Ahsan *et al.*, "Excursion-free dynamic wavelength switching in amplified optical networks," *IEEE/OSA J. Opt. Commun. Netw.*, vol. 7, no. 9, pp. 898–905, Sep. 2015.

[48] Y. Huang, P. B. Cho, P. Samadi, and K. Bergman, "Power excursion mitigation for flexgrid defragmentation with machine learning," *IEEE/OSA J. Opt. Commun. Netw.*, vol. 10, no. 1, pp. A69–A76, Jan. 2018.

[49] W. Mo *et al.*, "Deep-neural-network-based wavelength selection and switching in ROADM systems," *IEEE/OSA J. Opt. Commun. Netw.*, vol. 10, no. 10, pp. D1–D11, Oct. 2018.

[50] R. Luo, N. Hua, X. Zheng, and B. Zhou, "Fast parallel lightpath re-optimization for space-division multiplexing optical networks based on time synchronization," *IEEE/OSA J. Opt. Commun. Netw.*, vol. 10, no. 1, pp. A8–A19, 2018.

[51] X. Jin *et al.*, "Dynamic scheduling of network updates," *ACM SIGCOMM Comput. Commun. Rev.*, vol. 44, no. 4, pp. 539–550, Aug. 2014.

[52] Z. Zhu, W. Lu, L. Zhang, and N. Ansari, "Dynamic service provisioning in elastic optical networks with hybrid single-/multi-path routing," *J. Lightw. Technol.*, vol. 31, pp. 15–22, Jan. 1, 2013.

[53] G. Charlet *et al.*, "Transmission of 81 channels at 40Gbit/s over a transpacific-distance erbium-only link, using PDM-BPSK modulation, coherent detection, and a new large effective area fibre," in *Proc. ECOC*, Sep. 2008, pp. 1–2.

[54] M. Salsi *et al.*, "WDM 200 Gb/s single-carrier PDM-QPSK transmission over 12,000 km," in *Proc. ECOC*, Sep. 2011, pp. 1–3.

[55] M. Salsi *et al.*, "31 Tb/s transmission over 7, 200 km using 46 Gbaud PDM-8QAM with optimized error correcting code rate," in *Proc. OECC*, Jun./Jul. 2013, pp. 1–2.

[56] W. Idler, F. Buchali, and K. Schuh, "Experimental study of symbol-rates and MQAM formats for single carrier 400 Gb/s and few carrier 1 Tb/s options," in *Proc. OFC*, Mar. 2016, pp. 1–3.

[57] P. J. Winzer, "High-spectral-efficiency optical modulation formats," *J. Lightw. Technol.*, vol. 30, no. 24, pp. 3824–3835, Dec. 2012.

[58] Y. Wang, X. Cao, and Y. Pan, "A study of the routing and spectrum allocation in spectrum-sliced elastic optical path networks," in *Proc. IEEE INFOCOM*, Apr. 2011, pp. 1503–1511.

[59] H. Zhu, H. Zang, K. Zhu, and B. Mukherjee,, "A novel generic graph model for traffic grooming in heterogeneous WDM mesh networks," *IEEE/ACM Trans. Netw.*, vol. 11, no. 2, pp. 285–299, Apr. 2003.

[60] M. Jinno *et al.*, "Distance-adaptive spectrum resource allocation in spectrum-sliced elastic optical path network," *IEEE Commun. Mag.*, vol. 48, no. 8, pp. 138–145, Aug. 2010.

[61] B. Mukherjee, D. Banerjee, S. Ramamurthy, and A. Mukherjee, "Some principles for designing a wide-area WDM optical network," *IEEE/ACM Trans. Netw.*, vol. 4, no. 5, pp. 684–696, Oct. 1996.

[62] K. Zhu and B. Mukherjee, "Traffic grooming in an optical WDM mesh network," *IEEE J. Sel. Areas Commun.*, vol. 20, no. 1, pp. 122–133, Jan. 2002.

[63] S. Zhang, C. Martel, and B. Mukherjee, "Dynamic traffic grooming in elastic optical networks," *IEEE J. Sel. Areas Commun.*, vol. 31, no. 1, pp. 4–12, Jan. 2013.

[64] J.-F. P. Labourdette and A. S. Acampora, "Logically rearrangeable multihop lightwave networks," *IEEE Trans. Commun.*, vol. 39, no. 8, pp. 1223–1230, Aug. 1991.